from TEM mode to higher order modes is not affected. Thus, the energy converted from TEM mode to higher order modes is still lost, which determines the bandwidth of the modified TEM cell.

IV. Conclusion

Undesired higher order TE mode resonances limit the bandwidth of a TEM cell. A series of methods that can be used to suppress higher order TE modes has been proposed. A modified TEM cell with slotted walls, resistors between the traces, lossy absorbing materials wrapped around the cell, and an outer shielding box was designed and assembled. Measurements and the full-wave simulations demonstrate that the modified design is effective at suppressing the longitudinal magnetic field. The bandwidth of the modified TEM cell was increased to approximately 2.5 GHz, compared to 1 GHz for the original standard cell. The modified TEM cell can be used for radiated emission and immunity testing at frequencies up to 2.5 GHz.

References

[1] *Integrated circuits—Measurement of electromagnetic emissions, 150 kHz to 1 GHz—Part 2: Measurement of radiated emissions, TEM-cell and wideband TEM-cell method,* First ed., IEC 61967-2:2005, Sep. 2005.

[2] D. A. Hill, "Bandwidth limitations of TEM cells due to resonances," *J. Microw. Power*, vol. 18, no. 2, pp. 181–195, 1983.

[3] M. Koch, C. Groh, and H. Garbe, "Exact determination of resonant frequencies in TEM cells," in *Proc. 13th Int. Zurich Symp. Tech. Exhib. EMC*, Zurich, Switzerland, 1999, pp. 653–658.

[4] C. M. Weil and L. Gruner, "Higher order mode cutoff in rectangular striplines," *IEEE Trans. Microw. Theory Tech.*, vol. MTT-32, no. 6, pp. 638–641, Jun. 1984.

[5] C. Groh, H. Garbe, and M. Koch, "Higher order mode behavior in loaded and unloaded TEM cells," in *Proc. 1999 IEEE Int. Symp. Electromagn. Compat.*, Aug., vol. 1, pp. 225–230.

[6] C. Groh, J. P. Karst, M. Koch, and H. Garbe, "TEM waveguides for EMC measurements," *IEEE Trans. Electromagn. Compat.*, vol. 41, no. 4, pp. 440–445, Nov. 1999.

[7] D. Hansen and D. Ristau, "Characteristics of the EUROTEM family," in *Proc. 1999 Int. Symp. Electromagn. Compat.*, Tokyo, Japan, pp. 86–89.

[8] D. A. Hill and J. A. Walsh, "Resonance suppression in a TEM cell," *J. Microw. Power*, vol. 18, no. 4, pp. 325–330, 1983.

[9] M. L. Crawford, J. L. Workman, and C. L. Thomas, "Expanding the bandwidth of TEM cells for EMC measurements," *IEEE Trans. Electromagn. Compat.*, vol. EMC-20, no. 3, pp. 368–375, Aug. 1978.

[10] R. Lorch and G Monich, "Mode suppression in TEM cells," in *Proc. 1996 IEEE Int. Symp. Electromagn. Compat.*, Santa Clara, CA, Aug., pp. 40–42.

[11] P. F. Wilson and M. T. Ma, "Simple approximate expressions for higher order mode cutoff and resonant frequencies in TEM cells," *IEEE Trans. Electromagn. Compat.*, vol. EMC-28, no. 3, pp. 125–130, Aug. 1986.

[12] *HFSS 10.0 User's Guide,* Ansoft Corporation. Pittsburgh, PA, Jul. 2005.

[13] K. Ishihara and M. Tokuda, "Development of parallel wired cell," The Inst. Electron., Inf. Commun. Eng. (IEICE), Tokyo, Japan, Tech. Rep. EMCJ98-104-116, 1998.

[14] *CST Microwave Studio 5.1,* CST Computer Simulation Technology, Framingham, MA.

Using TEM Cell Measurements to Estimate the Maximum Radiation From PCBs With Cables Due to Magnetic Field Coupling

Shaowei Deng, Todd H. Hubing, *Fellow, IEEE*, and Daryl G. Beetner, *Senior Member, IEEE*

***Abstract*—Common-mode currents can be induced on cables attached to printed circuit boards (PCBs) due to electric and magnetic field coupling. This paper describes a technique for using transverse electromagnetic (TEM) cell measurements to obtain an effective common-mode voltage (or *magnetic moment*) that quantifies the ability of traces and integrated circuits on PCBs to drive common-mode currents onto cables due to magnetic field coupling. This equivalent common-mode voltage can be used to reduce the complexity of full-wave models that calculate the radiated emissions from a system containing the board. It can also be used without full-wave modeling to provide a relative indication of the likelihood that a particular board design will have unintentional radiated emissions problems due to magnetic field coupling.**

***Index Terms*—Magnetic field coupling, mutual inductance, radiated emissions, transverse electromagnetic (TEM) cell.**

I. Introduction

Common-mode currents are often a dominant source of unintentional radiated emissions from printed circuit boards (PCBs) [1]. Both electric field (capacitive) coupling and magnetic field (inductive) coupling can contribute significantly to the common-mode currents on cables attached to PCBs [2]. Models for estimating radiated emissions due to electric field coupling have been discussed in [3]. A magnetic field coupling model was presented in [4], and equations were developed to calculate this coupling for microstrip trace geometries.

The IEC 61967-2 standard [5] describes procedures for evaluating the emissions from integrated circuits (ICs) using a transverse electromagnetic (TEM) cell. The IC is mounted on a 10-cm square PCB that is secured to the wall of a TEM cell with the IC side facing into the cell, as shown in Fig. 1. The voltage measured on one end of the cell is used to evaluate the performance of the IC and the board. Recent studies [6], [7] have shown that the electric and magnetic field coupling from the IC can be isolated by measuring the output at both ends of the TEM cell and adding or subtracting the output voltages using a hybrid coupler. Electric field coupling measurements can be used to determine an "electric moment," which is a number that can be used to quantify the ability of the board to drive common-mode currents on attached cables due to electric field coupling [8]. This paper demonstrates how magnetic field coupling measurements made with a TEM cell can be used to determine a *magnetic moment* that can be used to quantify the ability of the board to drive common-mode current on attached cables due to magnetic field coupling.

II. Mutual Inductance in a TEM Cell

To illustrate how magnetic field coupling occurs between circuits on a PCB and a TEM cell, consider the microstrip trace geometry

Manuscript received August 8, 2007; revised October 26, 2007.

S. Deng was with the University of Missouri-Rolla, Rolla, MO 65409 USA. He is now with Juniper Networks, Sunnyvale, CA 94089 USA (e-mail: sdeng@juniper.net).

T. H. Hubing is with Clemson University, Clemson, SC 29634 USA (e-mail: hubing@clemson.edu).

D. G. Beetner is with the Missouri University of Science and Technology, Rolla, MO 65409 USA (e-mail: beetner@mst.edu).

Color versions of one or more of the figures in this paper are available online at http://ieeexplore.ieee.org.

Digital Object Identifier 10.1109/TEMC.2008.919026

0018-9375/$25.00 © 2008 IEEE

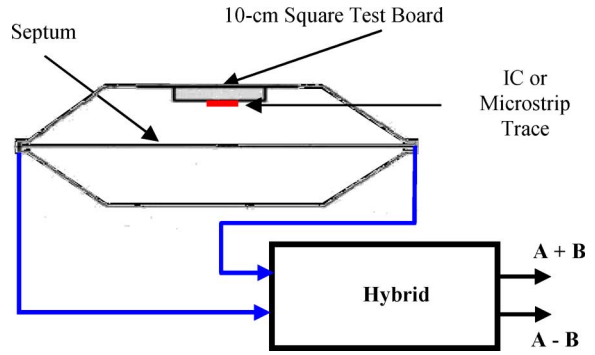

Fig. 1. Standard TEM cell measurement setup.

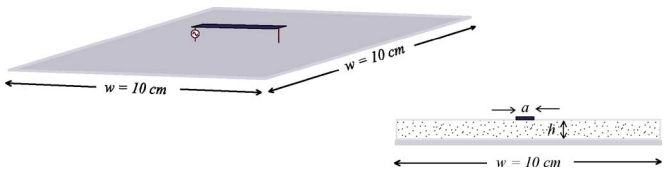

Fig. 2. Microstrip trace on a 10 cm × 10 cm board.

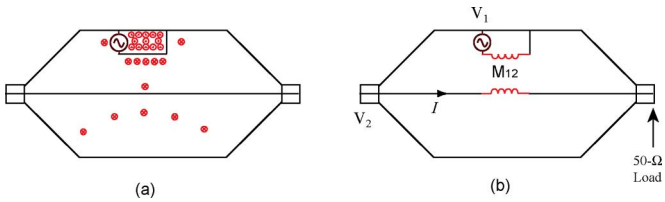

Fig. 3. Magnetic field coupling in a TEM cell.

illustrated in Fig. 2. The trace is located in the center of a 10 cm × 10 cm PCB. One end of the trace is shorted to the ground plane and a voltage source drives the other end. The dielectric between the trace and the ground plane has a relative permittivity of 4.4.

This board is mounted in the wall of a TEM cell with the shorted trace facing in. A voltage is applied to the trace through an SMA connector located on the backside of the board. The ground plane of the test board is shorted to the TEM cell outer wall.

Fig. 3 illustrates the magnetic field coupling mechanism in a TEM cell. Current flowing in the small microstrip loop generates a magnetic field in the cell. Some of the magnetic field lines wrap around the bottom side of the septum inducing a voltage between the septum and the wall of the cell. This voltage appears across both terminations with opposite phase. The voltage measured at the ports is proportional to the current in the loop and related to the ability of this loop to couple magnetic fields to the septum. This magnetic field coupling can be represented by a mutual inductance, M, between the source loop and the septum-cell loop, as indicated in the figure. The transfer coefficient S_{21} between the hybrid "A–B" port and the SMA connector on the test board is measured using a network analyzer. The measured S_{21} can be used to calculate the magnetic field coupling from the microstrip loop to the TEM cell [6].

The current flowing in the septum is related to the voltage at a termination by the 50-Ω impedance of the TEM cell

$$|I| = \left|\frac{V_1}{Z_0}\right|. \tag{1}$$

TABLE I
MEASURED AND CALCULATED MUTUAL INDUCTANCE IN THE TEM CELL

Microstrip trace geometry	Trace length l (mm)	Board thickness h (mm)	Trace width a (mm)	Measured M using Equation (6)	Numerically Calculated M using Q3D
Short trace	21	1.4	2	0.09 nH	0.08 nH
Long trace	32	1.6	2	0.14 nH	0.13 nH

This current generates a magnetic flux density

$$|\boldsymbol{B}| = \frac{\mu_0 |I|}{2(W+H)} \tag{2}$$

near the wall of the TEM cell, where W is the width of the TEM Cell and H is the height of the TEM cell. The amount of magnetic flux coupled to the small microstrip loop on the test board is approximately

$$\Phi_{21} \approx |\mathbf{B}| \cdot l \cdot h = \frac{\mu_0 |I| lh}{2(W+H)} \tag{3}$$

where l is the length of the microstrip trace and h is the thickness of the PCB dielectric. The mutual inductance in the TEM cell can be determined by

$$M = \frac{\Phi_{21}}{|I|} = \frac{\mu_0 lh}{2(W+H)}. \tag{4}$$

S_{21} obtained in the TEM cell measurement can be related to the magnetic flux flowing through the small microstrip loop by

$$|S_{12}| = |S_{21}| = \left|\frac{V_2}{V_1}\right| = \left|\frac{\omega\Phi_{21}}{V_1}\right|. \tag{5}$$

Thus, from the definition of the mutual inductance and (1) and (5), one can derive (6) to estimate the mutual inductance value from the TEM cell measurement

$$M = \left|\frac{\Phi_{21}}{I}\right| = \left|\frac{S_{21}V_1}{\omega I}\right| = \frac{|S_{21}|}{2\pi f} \times Z_0. \tag{6}$$

Note that the measured $|S_{21}|$ is nearly proportional to frequency over the frequency range of interest, so the measured value of M is a constant. Two microstrip boards were measured in a TEM cell using this method and the mutual inductance values obtained using (6) are shown in Table I. The mutual inductance values were also calculated using a 3-D static field solver [9] and the measured mutual inductance values agree well with the calculated results for both microstrip boards.

III. COMMON-MODE INDUCTANCE

When there are cables attached to the microstrip board, the magnetic flux that wraps around the current return plane can induce a common-mode voltage between the cables resulting in significant radiated emissions. This common-mode voltage is proportional to the product of a "common-mode inductance," L_{CM}, and the differential mode current in the loop [4]. The common-mode inductance represents the mutual inductance between the source loop and the "antenna" formed by the return plane and attached cables. An equivalent circuit model illustrating the common-mode inductance for the microstrip board is shown in Fig. 4.

An approximate equation for estimating the common-mode inductance for the microstrip structure is presented in [4]

$$L_{\mathrm{CM}} = \frac{4\mu_0 hl}{\pi^2 w} \tag{7}$$

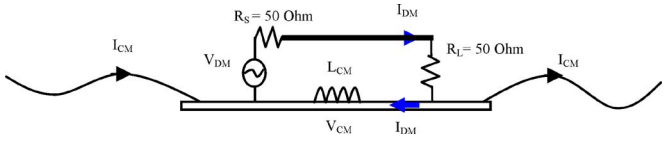

Fig. 4. Simple configuration illustrating common-mode radiation.

TABLE II
COMMON-MODE INDUCTANCE OF TWO MICROSTRIP GEOMETRIES

	L_{CM} calculated using Equation (7) for known microstrip geometry	L_{CM} calculated using Equation (11) from measured M in a TEM cell
Short trace	0.15 nH	0.17 nH
Long trace	0.26 nH	0.27 nH

where w is the width of the test board. The effective common-mode voltage that drives the attached cables is

$$V_{\mathrm{CM}} = \omega L_{\mathrm{CM}} I_{\mathrm{DM}}. \tag{8}$$

In the TEM cell measurement, the differential-mode current, I_{DM}, flowing in the trace induces a voltage at both ports of the TEM cell

$$V_{\mathrm{TEM}} = \omega I_{\mathrm{DM}} M. \tag{9}$$

Substituting (4), (7), and (9) into (8)

$$\begin{aligned} V_{\mathrm{CM}} &= \omega L_{\mathrm{CM}} I_{\mathrm{DM}} \\ &= \frac{4\mu_0 hl}{\pi^2 w} \times \frac{V_{\mathrm{TEM}}}{M} \\ &= \frac{4}{\pi^2 w} \times V_{\mathrm{TEM}} \times 2(W+H). \end{aligned} \tag{10}$$

Thus, the common-mode inductance L_{CM} is

$$L_{\mathrm{CM}} = M \frac{V_{\mathrm{CM}}}{V_{\mathrm{TEM}}} = M \frac{4 \cdot 2(W+H)}{\pi^2 w}. \tag{11}$$

The common-mode inductance, L_{CM}, can therefore be determined by measuring the mutual inductance between the microstrip trace and the septum of a TEM cell without knowing the microstrip trace geometry. Values of L_{CM} obtained from TEM cell measurements using (11) are compared with the calculated results obtained using (7), as shown in Table II for the 21- and 32-mm traces studied earlier. There is good agreement between the calculated and measured results.

IV. RADIATED EMISSIONS

The maximum radiated emissions from boards with two 50-cm cables attached were investigated for both the 21-mm trace board and the 32-mm trace board. The boards with attached cables were modeled as dipole antennas, as shown in Fig. 5. The equivalent common-mode source amplitude was

$$V_{\mathrm{CM}} = \omega I_{\mathrm{DM}} L_{\mathrm{CM}} = 2\pi f \times \frac{V_{\mathrm{DM}}}{R_S + R_L} \times L_{\mathrm{CM}}. \tag{12}$$

V_{CM} is effectively a "magnetic moment" analogous to the "electric moment," described in [8]. It quantifies a board's ability to drive attached cables or enclosures through magnetic field coupling just as the electric moment quantifies a board's ability to drive cables or enclosures due to electric field coupling. Like the electric moment, the magnetic moment can be determined from a hybrid TEM cell measurement directly, without making prior assumptions about the loop currents or geometry.

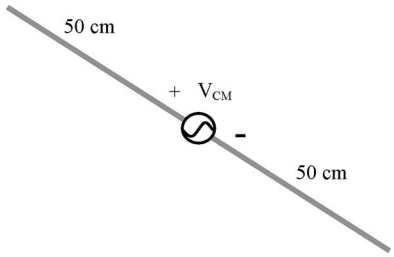

Fig. 5. Dipole antenna model with equivalent voltage source representing the magnetic field coupling.

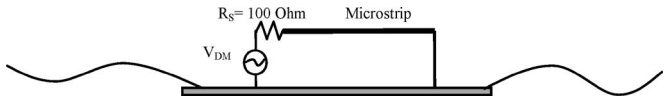

Fig. 6. Equivalent inductive coupling model for the microstrip board.

Fig. 6 illustrates the first microstrip board geometry evaluated. One end of the microstrip trace is shorted to the ground plane in order to maximize the magnetic field coupling and minimize the electric field coupling from the trace.

The maximum far-field radiation at a distance of 3 m was calculated using a full-wave simulation tool [10]. The full-wave simulation results for the 21- and 32-mm microstrip traces using the equivalent inductive coupling model are indicated by the dashed lines in Fig. 7(a) and (b), respectively. The corresponding estimates of the maximum radiated emissions due to inductive coupling using the TEM cell measurements and the equivalent dipole model in Fig. 5 are indicated by the solid lines in these figures. The equivalent common-mode voltage source was calculated using (12). The common-mode inductance was calculated using (11) from TEM cell measurements. For both microstrip structures, the estimates made using the dipole model and V_{CM} measured in the TEM cell agree well with the full-wave simulation results (i.e. within a few decibels from 30 MHz to 300 MHz).

When the trace is terminated with a 50-Ω resistance, as shown in Fig. 4, the radiated emissions include both inductive and capacitive coupling components. The capacitive (electric-field) coupling can be isolated in these microstrip structures by modeling the traces with open terminations.

Full-wave simulation results showing the maximum 3-m radiation from the microstrip traces terminated with 50-Ω are indicated by the solid lines in Fig. 8(a) and (b) for the 21- and the 32-mm traces, respectively. The maximum emissions due to inductive coupling, as determined by the TEM cell technique described here, are indicated by the uniform dashed line. The emissions due to capacitive coupling, based on a full wave analysis of the open-circuit configuration, are indicated by the dashed-dotted line. (A procedure for estimating the maximum capacitive coupling based on TEM cell measurements is presented in [8].) For the 50-Ω terminated traces, both capacitive coupling and inductive coupling contribute significantly to the overall radiated emissions.

V. DISCUSSION

For the simple microstrip structures investigated in this paper, it is possible to calculate the mutual inductance M and common-mode inductance L_{CM} from a TEM cell measurement, since the current on the trace is known. For a PCB with unknown IC and trace geometries, a single TEM cell measurement cannot be used to determine both the

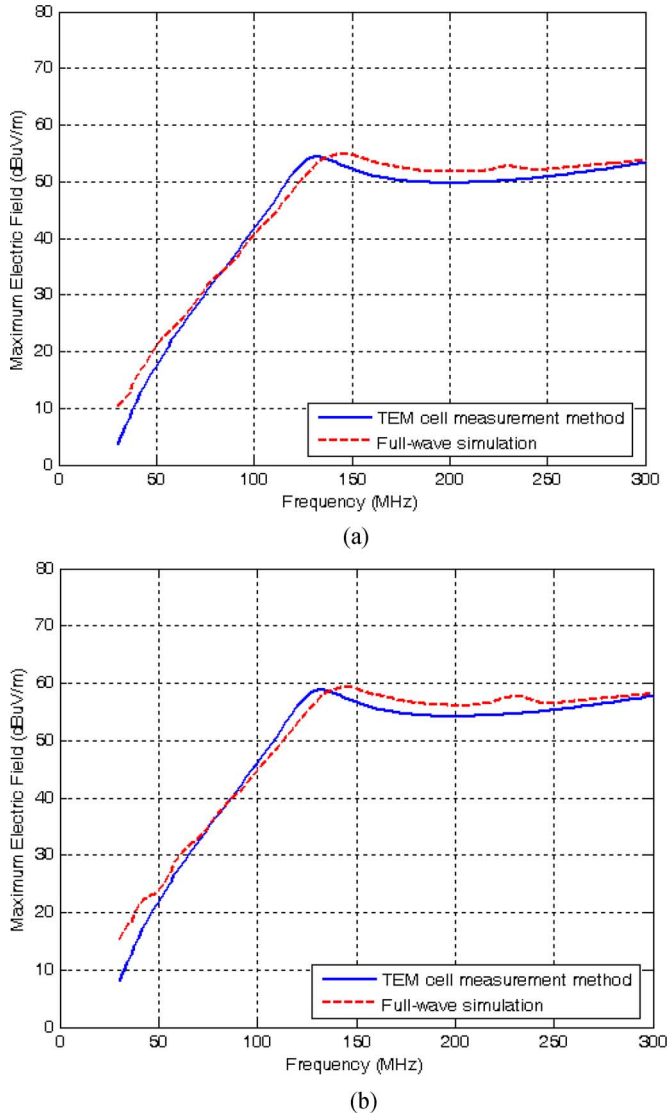

Fig. 7. Inductive coupling for (a) the 21-mm and (b) 32-mm microstrip trace.

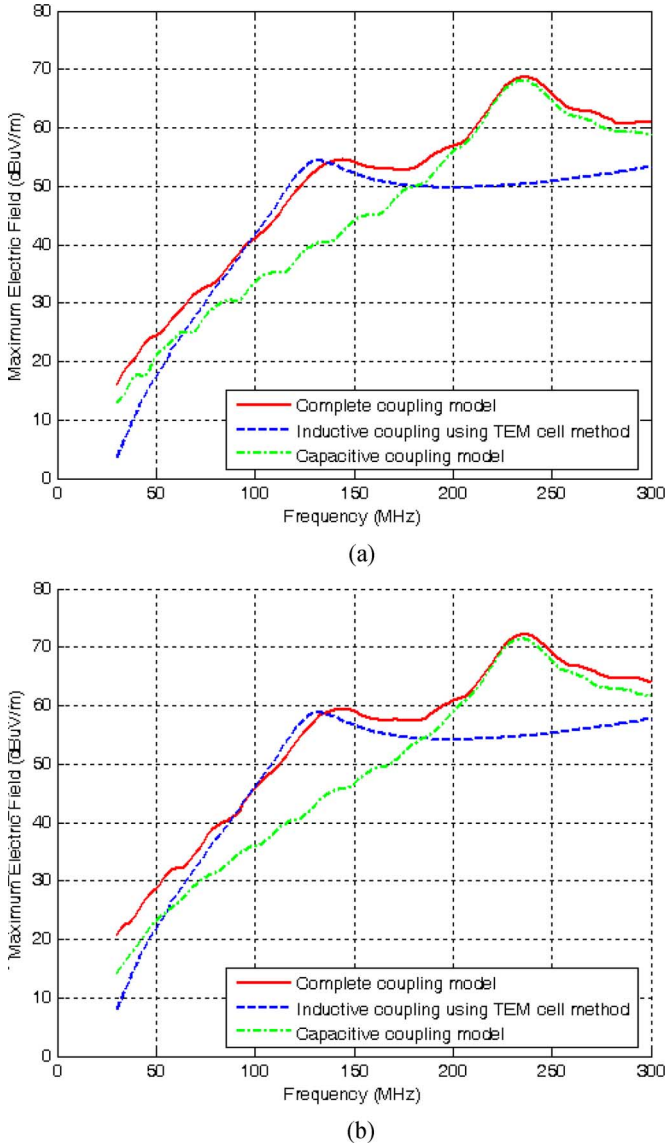

Fig. 8. Far-field radiation for (a) the 21-mm and (b) 32-mm microstrip trace.

current and the common-mode inductance independently. However, as shown in (9) and (10), the TEM cell measurement does yield the product of these quantities. The product is sufficient to determine the magnetic moment, which is essentially the equivalent common-mode voltage developed across the board due to magnetic field coupling.

The technique presented here is valid for PCBs with any geometry so long as the board and the source loops are electrically small. If there are multiple current loops on a board, the measured common-mode voltage will be the magnitude of the vector sum of the contributions from each current loop. Therefore, an electrically small board with many components and traces can be evaluated in a TEM cell and a single common-mode voltage (as a function of frequency) can be obtained that represents the ability of that board to inductively couple common-mode currents onto attached cables.

Since the magnetic field coupling to the septum is a function of the board orientation, the magnetic moment will also be a function of board orientation. It is relatively easy, however, to determine the maximum possible coupling from the measurement of two perpendicular board orientations. In this way a single value for the maximum magnetic moment can be obtained.

VI. Conclusion

A simple method for using TEM cell measurements to obtain an equivalent common-mode voltage that represents a circuit board's ability to inductively couple to attached cables has been presented. In full-wave models, where the goal is to determine the radiated emissions due to magnetic field coupling, significant computational resources can be saved by replacing the complex circuit geometries on the board with a single voltage source. In this paper, the radiated emissions from two boards with microstrip traces and attached cables were estimated with good accuracy using this method.

However, even if full-wave modeling is not performed, the common-mode voltage obtained from this type of TEM cell measurement can be helpful. It provides a relative indication of the strength of the board as a magnetic field coupling source. Also, with the help of simple worst case antenna models, this common-mode voltage can be used to estimate the worst case radiated emissions due to magnetic field coupling that could occur when a particular board is installed in a system.

REFERENCES

[1] C. Paul, "A comparison of the contributions of common-mode and differential-mode currents in radiated emissions," *IEEE Trans. Electromagn. Compat.*, vol. 31, no. 2, pp. 189–191, May 1989.

[2] D. Hockanson, J. Drewniak, T. Hubing, T. Van Doren, F. Sha, and M. Wilhelm, "Investigation of fundamental EMI source mechanisms driving common-mode radiation from printed circuit boards with attached cables," *IEEE Trans. Electromagn. Compat.*, vol. 38, no. 4, pp. 557–566, Nov. 1996.

[3] H. W. Shim and T. H. Hubing, "Model for estimating radiated emissions from a printed circuit board with attached cables driven by voltage-driven sources," *IEEE Trans. Electromagn. Compat.*, vol. 47, no. 4, pp. 899–907, Nov. 2005.

[4] D. M. Hockanson, J. L. Drewniak, T. H. Hubing, T. P. Van Doren, F. Sha, C. Lam, and L. Rubin, "Quantifying EMI resulting from finite-impedance reference planes," *IEEE Trans. Electromagn. Compat.*, vol. 39, no. 4, pp. 286–297, Nov. 1997.

[5] *Integrated Circuits—Measurement of Electromagnetic Emissions, 150 kHz to 1 GHz—Part 2: Measurement of Radiated Emissions, TEM-Cell and Wideband TEM-Cell Method,* IEC 61967-2:2005, 1st ed., Sep. 2005.

[6] V. Kasturi, S. Deng, T. Hubing, and D. Beetner, "Quantifying electric and magnetic field coupling from integrated circuits with TEM cell measurements," in *Proc. 2006 IEEE Int. Symp. Electromagn. Compat.*, Portland, OR.

[7] A. Nakamura, "EMC basic series no. 21: Measurement methods and applications of electromagnetic emission of semiconductor devices," *J. Jpn. Inst. Electron. Packag.* (in Japanese), vol. 6, no. 4, pp. 344–351, 2004.

[8] S. Deng, T. Hubing, and D. Beetner, "Characterizing the electric-field coupling from IC-heatsink structures to external cables using TEM-cell measurements," *IEEE Trans. Electromagn. Compat.*, vol. 49, no. 4, pp. 785–791, Nov. 2007.

[9] *Q3D Extractor Version 7.0 User's Guide*, Ansoft Corporation, Pittsburgh, PA, Aug. 2005.

[10] *CST Computer Simulation Technology, CST Microwave Studio 5.1,* CST, Darmstadt, Germany.

High-Frequency Common-Mode Modeling of Permanent Magnet Synchronous Motors

Kayhan Gulez, *Member, IEEE*, and Ali A. Adam

***Abstract*—In this paper, a model for permanent magnet synchronous motors to deal with high-frequency emissions from an inverter system is proposed and analyzed. The model permits study of the common-mode (CM) effects on the motor line currents. The experimental measurements show that the CM stray capacitors are not affected by rotor magnet positions. The simulated and experimental results show that the CM currents increase with decreasing sampling time.**

***Index Terms*—Common mode (CM), electromagnetic interference (EMI) noise, high-frequency model, motor control, permanent magnet synchronous motor (PMSM) model.**

I. INTRODUCTION

Due to their high power density and high torque/inertia ratio, permanent magnet synchronous motors (PMSMs) are widely used in high-performance drives, such as electrical vehicles and robotic applications. The controlling of the speed or torque of a PMSM usually follows either field-oriented control (FOC) or the most popular direct torque control (DTC).

Although these methods normally satisfy the required control goal, they have many disadvantages such as switching and current harmonics supplied by the power inverter that is updated only once when the outputs of the hysteresis controllers change states. These harmonics cause many unwanted phenomena including electromagnetic interference (EMI), parasitic torque pulsation, and the associated mechanical vibration and acoustic noise.

In order to understand such parasitic effects, desired currents have to be distinguished from parasitic currents in a suitable mathematical model. Undesired current components can flow in both common mode (CM) and differential mode paths [1]. CM currents flow from stray capacitors that exist between many parts of the system, through earth ground and back to the ac power main, through its ground connection. Differential mode currents flow out and return through the phase conductors, i.e., the required signal and the differential mode noise take the same path that makes it difficult to be interpreted. In the literature, several researches efforts [1]–[10] have been carried out to model induction motor–inverter–feeding cable systems with different degrees of success; for example, in [2]–[4], differential and CM modeling have been achieved to correct motor model at high frequency and to deal with shaft voltages and bearing currents due to the CM. High-frequency modeling in [5] and [6] for both a long cable and an induction motor has been achieved to deal with over voltages due to the wave reflection, and in [7], simulated results have been introduced to deal with suppression of the inverter's adverse effect including EMI noise. However, no research efforts have been dedicated to deal with PMSM high-frequency response.

This paper proposes a high-frequency common-mode model for PMSM. The proposed model addressing a wide high-frequency range can be useful to observe EMI noise, and assist in modeling suitable EMI filters whose design depends on whether CM or differential mode noise has to be reduced.

Considering the possible high-frequency signals penetrating through the motor frame and windings, the proposed modeling procedure consists of a set of measurements at different frequencies to get the impedance responses of the CM path.

II. EXPERIMENTAL MODELING OF PMSM

The measurement setup is composed of an oscilloscope with voltage and current probes, and a small signal generator that is used to inject high-frequency sinusoidal voltage into the motor windings. Through inspection of the measured impedance behavior, it is possible to infer the motor model for high frequencies. The experimental measurements were performed in the range 10 kHz to 20 MHz for the CM calculations.

The PMSM are normally modeled in the in rotor reference frame are given as

$$\begin{bmatrix} v_{sd} \\ v_{sq} \end{bmatrix} = \begin{bmatrix} R_s + pL_{sd} & -P\omega_r L_{sq} \\ P\omega_r L_{sd} & R_s + pL_{sq} \end{bmatrix} \begin{bmatrix} i_{sd} \\ i_{sq} \end{bmatrix} + \begin{bmatrix} 0 \\ e_B \end{bmatrix} \quad (1)$$

where v_{sd} and v_{sq} are the d-axis and q-axis stator voltages, i_{sd} and i_{sq} are the d-axis and q-axis stator currents, R_s is the stator winding resistance, L_{sd} and L_{sq} are the d-axis and q-axis stator inductances, $p = d/dt$ is the differential operator, P is the number of pole pairs of the motor, ω_r is the rotor speed, Ψ_F is the rotor permanent magnetic flux, and $e_B = P\omega_r \Psi_F$ is the generated back emf due to Ψ_F.

Manuscript received May 8, 2007; revised October 1, 2007.

K. Gulez is with the Electrical Engineering Department, Yildiz Technical University, 34349 Istanbul, Turkey (e-mail: gulez@yildiz.edu.tr).

A. A. Adam was with the Electrical Engineering Department, Yildiz Technical University, 34349 Istanbul, Turkey. He is now with the Faculty of Engineering Science, Omdurman Islamic University, Omdurman 24915, Sudan (e-mail: aliadam999@yahoo.com).

Color versions of one or more of the figures in this paper are available online at http://ieeexplore.ieee.org.

Digital Object Identifier 10.1109/TEMC.2008.921032

0018-9375/$25.00 © 2008 IEEE